EXPERIMENTAL ANALYSIS OF ACTIVE-PASSIVE VIBRATION CONTROL USING EXTENSION AND SHEAR PIEZOELECTRIC ACTUATORS

Marcelo Areias Trindade
Rafael Picolo Gonzaga de Azevedo
Pedro Henrique de Marques Guatura
Department of Mechanical Engineering, São Carlos School of Engineering, University of São Paulo, Av. Trabalhador São-Carlense, 400, São Carlos, SP 13566-590, Brazil, trindade@sc.usp.br

Abstract. *Hybrid active-passive damping treatments combine the reliability, low cost and robustness of viscoelastic damping treatments and the high performance, modal selective and adaptive piezoelectric active control. Numerous hybrid damping treatments have been reported in the literature. They differ mainly by the relative positions of viscoelastic treatments, sensors and piezoelectric actuators. This work presents an experimental analysis of three active-passive damping design configurations applied to a cantilever beam. In particular, two design configurations based on the extension mode of piezoelectric actuators combined to viscoelastic constrained layer damping treatments and one design configuration with shear piezoelectric actuators embedded in a sandwich beam with viscoelastic core are analyzed. For comparison purposes, a purely active design configuration with an extension piezoelectric actuator bonded to an elastic beam is also analyzed. The active-passive damping performance of the four design configurations is compared. Results show that active-passive design configurations provide more reliable and wider-range damping performance than purely active one.*

Keywords: *Active-passive vibration control, piezoelectric materials, viscoelastic materials, shear piezoelectric actuators, sandwich structures*

1. INTRODUCTION

Several research works published in the last decade have shown the advantages of combining the standard free layer and constraining layer viscoelastic damping treatments with some type of distributed active control to reduce the structural vibration amplitudes. The viscoelastic damping treatments offer a reliable, low cost and robust solution for vibration damping and are already widely used in several industries. On the other hand, studies on the application of distributed active control using piezoelectric actuators for real structures has seen a considerable growth in recent years. Although a purely active control is normally not robust enough for industrial applications, it can provide high performance, modal selective and adaptive solutions for narrow frequencies ranges. Aiming to improve passive damping performance or reduce the required weight increase, a number of research groups proposed hybrid active-passive damping treatments configurations combining both viscoelastic and piezoelectric materials in the structural design (Lam, Inman and Saunders, 1998; Trindade and Benjeddou, 2002).

Depending on the relative positions of the passive damping layers and the active piezoelectric actuators, the active and passive damping mechanisms can work separately or simultaneously. The most studied configuration consists of replacing or augmenting the elastic constraining layer of a Passive Constrained Layer (PCL) damping treatment by an active piezoelectric actuator, leading to the so-called Active Constrained Layer (ACL) (Baz and Ro, 1994; Huang, Inman and Austin, 1996; Lesieutre and Lee, 1996) or Active-Passive Constrained Layer (APCL) damping treatments (Azvine, Tomlinson and Wynne, 1995). The APCL construction allows different lengths for active and passive treatments, unlike ACL in which actuators entirely cover viscoelastic layers. Alternative configurations to ACL/APCL, mainly separating the passive treatment of the active piezoelectric actuators, were later proposed (Lam, Inman and Saunders, 1998; Trindade and Benjeddou, 2002). It was shown that, although each configuration has its advantages, the active damping performance is very much dependent on the transmissibility between piezoelectric actuators and host beam. Hence, ACL design can only be an interesting design when active and passive damping are designed to operate complementarily.

To remedy for the transmissibility reduction of ACL/APCL, Liao and Wang (1996) suggested to add rigid elements at the actuators edges to connect them directly to the structure. This treatment, named Enhanced ACL, allows to improve active control but reduces passive damping. This configuration was also studied by Varadan, Lim and Varadan (1996), Badre-Alam, Wang and Gandhi (1999) and Chan and Liao (2006). Another solution to increase transmissibility is to consider active and passive treatments acting separately. Thus, Crassidis, Baz and Wereley (2000) proposed to bond a piezoelectric actuator directly on the bottom surface of a beam, in addition to an ACL treatment bonded on the opposite surface. Lam, Inman and Saunders (1998) presented separate active (AC) and passive (PCL) treatments, bonded on the same side and on the opposite sides of a beam, leading to the so-called AC/PCL treatments. Their results showed that the two AC/PCL treatments are more effective and require less control voltages than the ACL, specially when active and passive treatments are placed on the opposite sides. Lam, Inman and Saunders (1998) and Trindade and Benjeddou (2002)

suggested to place the piezoelectric actuator underneath the viscoelastic material, leading to better passive damping. This allows direct AC action and Passive Stand-Off Layer (PSOL) damping. Hence, this treatment is named AC/PSOL. Alternatively, Trindade, Benjeddou and Ohayon (2001) and Wang, Veeramani and Wereley (2000) proposed to actuate a sandwich beam with viscoelastic core by using surface-bonded piezoelectric actuators, although only in the first work the piezoelectric actuators were used to provide an active-passive damping. Recently, Baillargeon and Vel (2005) studied a sandwich beam with shear piezoelectric actuators embedded in its core, although they have focused on the active damping mechanism only. A geometric and topological optimization of these active-passive damping designs, accounting for the treatments cited above, was recently published (Trindade, 2007).

An analysis of the experimental studies published in the literature shows that the hybrid constrained layer treatments are generally applied to very thin structures, thus very flexible. This has justified the choice of a Bernoulli-Euler (Kirchoff) model for the host structures on the major part of the studies published. In addition, studies related to beam structures generally consider cantilever beams. The hybrid treatments themselves are generally very thin covering about 60-70% of the host structure, increasing the thickness and the volume of the resulting structure by around 60% and 30% respectively. It is known that constrained layer treatments are more effective when the bending stiffness of the constraining layer is of the same order as that of the host structure. However, it was generally taken as only about 30% of that of the host structure. This is clearly due to the thickness limitations of an added treatment to existing structures. On the other hand, the added active control effectiveness to a pure passive constrained layer treatment of hybrid treatments allows to overcome part of this limitation. Also, the viscoelastic layers considered in these hybrid treatments are generally very thin. This is justified by several facts. First, passive constrained layer treatments are normally more effective to control several vibration modes when using very thin viscoelastic layers. Second, it is known that ACL/APCL treatments suffer from lost transmissibility between the actuator and the host structure due to the softness of the viscoelastic layer (Rongong et al., 1997). The thickness-to-length ratio of the viscoelastic layers is also generally very small, around 0.1%. However, due to the structure construction, these layers are normally subjected to shear strains and hence they cannot be modelled as Bernoulli-Euler beams.

The majority of the publications, concerning experimental studies, shows very simple control strategies applied to hybrid damping treatments, such as piezoelectric control voltages proportional to the displacement or the velocity of a particular point of the structure. Some authors (Azvine, Tomlinson and Wynne, 1995; Crassidis, Baz and Wereley, 2000; Kapadia and Kawiecki, 1997; Langote and Seshu, 2005) have preferred to measure the displacement of some point in the structure, others, the acceleration (Ray, Oh and Baz, 2001), and then evaluate numerically the corresponding velocity. Other authors preferred to apply control voltages proportional to the voltage induced on a piezoelectric sensor, or its derivative (Baz and Ro, 2001; Park and Baz, 2001; Yellin and Shen, 1996). Recently, Vasques and Dias Rodrigues (2007) proposed to feed back directly after amplification the velocity measured by a laser vibrometer. The main advantage of such simple control strategies is that they do not require a very refined structural model nor demand complex signal processing. Nevertheless, some authors did account for more complex control strategies as an optimal LQG (Chantalakhana and Stanway, 2000).

This work presents experimental results for the damping performance of three active-passive damping treatments applied to cantilever beams. Two design configurations based on the extension mode of piezoelectric actuators combined to viscoelastic constrained layer damping treatments, APCL and AC/PCL, and one design configuration with shear piezoelectric actuators embedded in a sandwich beam with viscoelastic core are analyzed. For comparison purposes, a purely active design configuration with an extension piezoelectric actuator bonded to an elastic beam is also analyzed. The active-passive damping performance of the four design configurations is compared.

2. EXPERIMENTAL SETUP

2.1 Active-passive damping treatments configurations

The three active-passive and the active damped cantilever beams are shown in Fig. 1. They were constructed using aluminum sheets with length 280 mm, width 25 mm and thickness 3 mm.

The actively damped beam (Fig. 1a), named Extension Active (EA), was obtained by bonding a transversely poled, or extension, PIC151 piezoceramic patch (PI Ceramic) on one of the surfaces of the beam using an epoxy-based glue (Araldite) cured at 60^{o}C. The piezoceramic patch has length 25 mm, width 25 mm and thickness 0.5 mm and was bonded at 70 mm of the aluminum sheet left end. The beam with bonded piezoceramic patch is then clamped, using two bolted thick steel plates fixed to a heavy concrete block, such that the cantilever section is 220 mm long and the piezoceramic patch is located at 10 mm of the clamp, as shown in Fig. 1a.

The first active-passive design considered is the Active-Passive Constrained Layer (APCL), shown in Fig. 1b, which consists of two patches of SD40 viscoelastic material (EAR Specialty Composites) constrained by one aluminum sheet each, where the left aluminum constraining layer has a bonded PIC151 piezoceramic patch (Fig. 1b). Each viscoelastic layer has thickness 0.7 mm and the aluminum constraining layers are 1 mm thick. The four layers have length 60 mm and width 25 mm. The bonding of the piezoceramic patch on the 1 mm aluminum sheet followed the same procedure

described above (cured Araldite). The bonding of the viscoelastic layers on the 3 mm and 1 mm aluminum beam was performed using non-cured Araldite. As shown in Fig. 1b, the two treatments were bonded such that, after clamping, they are located at a 10 mm and 125 mm distance from the clamp.

A variation of this design configuration is shown in Fig. 1c, so-called Active Control/Passive Constrained Layer (AC/PCL), where the piezoceramic patch is bonded on one side of the beam and the two constrained viscoelastic layers on the opposite side. This design was constructed bonding the two constrained viscoelastic layers to another specimen of the beam shown in Fig. 1a. This bonding was also performed using a non-cured Araldite.

The last active-passive design configuration, shown in Fig. 1d and named Shear Active-Passive (SAP), is a sandwich construction with two 3 mm aluminum facings. The sandwich core is composed of a longitudinally poled, or shear, PIC255 piezoceramic patch (PI Ceramic) and two layers of a viscoelastic double coated polyethylene foam tape (3M 4494), as shown in Fig. 1d. The foam tape has thickness 1 mm and width 25 mm. The piezoceramic patch is 0.5 mm thick but this thickness increases to approximately 0.8 mm after cabling of the top and bottom electrodes. The shear piezoceramic patch was bonded to the top and bottom aluminum facings with Araldite cured at 60°C. To withstand the large clamping force of the bolts, a 1 mm aluminum sheet was used for the 60 mm long clamped section core.

(a) Extension Active (EA)

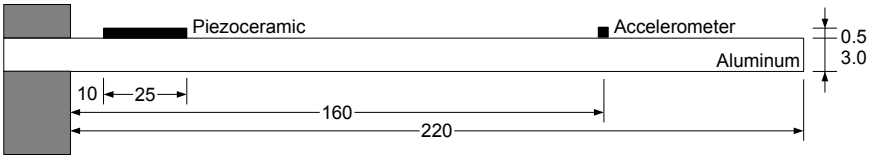

(b) Active-Passive Constrained Layer (APCL)

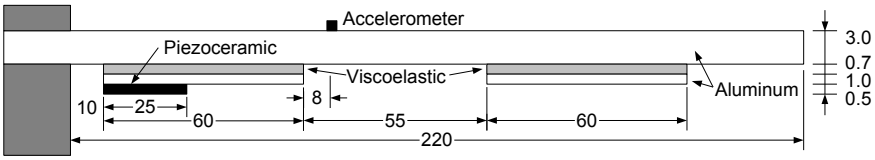

(c) Active Control/Passive Constrained Layer (AC/PCL)

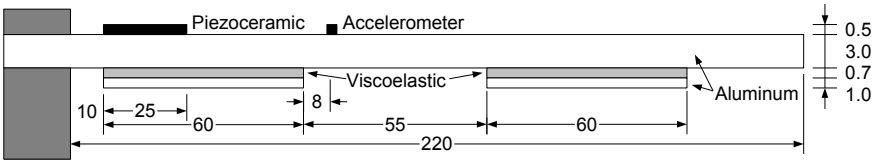

(d) Shear Active-Passive (SAP)

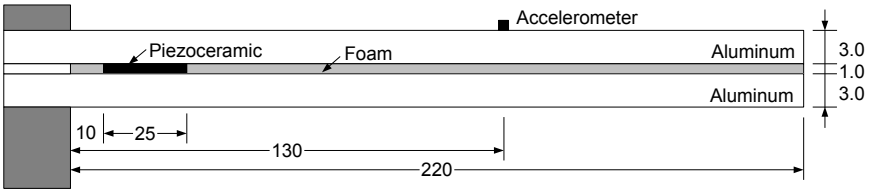

Figure 1. Schematic representation of the cantilever beams with EA, APCL, AC/PCL and SAP damping treatments (dimensions in mm and not in scale).

The four configuration designs are depicted in Fig. 2, where the picture of the SAP configuration was zoomed so that one could observe the embedded piezoceramic shear actuator (Fig. 2d).

2.2 Data acquisition and signal processing

A general schematic representation and picture of the experimental setup are depicted in Fig. 3. An accelerometer (Brüel&Kjær 4375) was considered for both measurement and observation of the structural response and feedback control. Its placement was optimized to provide a satisfactory reading of the structural response and to improve the active control performance of each configuration (Fig. 1). The accelerometer output is passed through a signal conditioner (Brüel&Kjær 2626) before acquisition. The structure is both excited and controlled using the piezoceramic patch, i.e. the active element of each configuration. For that, two independent signals are sent to the piezoceramic patch as described later on. Since piezoceramic actuators require relatively high voltages to provide satisfactory actuation performance, a power amplifier

(a) Extension Active (EA)

(c) Active Control/Passive Constrained Layer (AC/PCL)

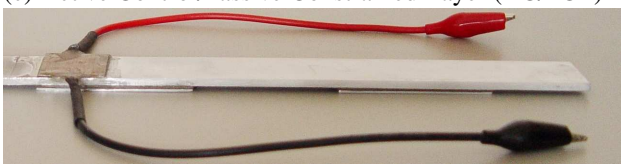

(b) Active-Passive Constrained Layer (APCL)

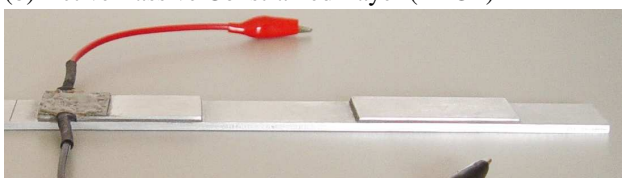

(d) Shear Active-Passive (SAP)

Figure 2. Pictures of the cantilever beams with EA, APCL, AC/PCL and SAP damping treatments.

(Midé EL-1224) with a gain 20 V/V was used to connect the dSPACE output to the piezoceramic patches. The dSPACE connector panel (CLP) input and output connectors are limited to ± 10 V. Hence, a maximum voltage amplitude of 200 V could be applied to the piezoceramic patches. Since the piezoceramic patches are 0.5 mm thick, this leads to an electric field magnitude up to 400 V/mm, which is sufficient to achieve significant actuation forces. Both accelerometer input and piezoceramic output signals were processed using a DS1104 dSPACE control system connected to a PC. This allows to implement both signal processing and control law using Simulink models which are then compiled through Real Time Workshop and uploaded in the dSPACE controller board.

The Simulink model used for the signal processing and control law implementation is shown in Fig. 4. It consists of four main groups of blocks: 1) acquisition, filtering and integration of accelerometer signal to provide a clean transverse velocity measurement at the accelerometer location; 2) evaluation of the control voltage to be applied to the piezoceramic patch using a simple direct velocity feedback law, where the control gain can be chosen afterwards, followed by a controlled saturation to avoid uncontrolled saturation of the combined voltage signals at the dSPACE connector panel; 3) setup of the excitation voltage signal to be applied to the piezoceramic patch, for which a chirp signal was used; and 4) output of combined voltage signals, to be applied to the piezoceramic patch, to the dSPACE connector panel. Some issues regarding the Simulink model deserve discussion. In particular, the high-pass filtering of the accelerometer signal was used mainly to eliminate the DC component and thus a simple second-order Butterworth high-pass filter with a cutoff frequency of 50 rad/s was considered. In order to allow independent excitation and control through the piezoceramic patch and avoid uncontrolled saturation, the control voltage signal saturation was set up to 150 V while the chirp excitation voltage, limited to 45 V, was defined by manually adjusting the chirp gain so that the structural response measurement was optimized for each configuration. A sampling time of 50 μs was considered for the acquisition.

Using the compiled model uploaded in the dSPACE controlled board, a series of measurements were performed for each design configuration to determine satisfactory parameters of the data acquisition, signal processing, accelerometer location and piezoceramic patches control gains. To qualify the measurements and the damping performance, the frequency response function (FRF) between the chirp excitation voltage and the transverse velocity at the accelerometer location was evaluated. For that, a routine was developed in MATLAB to process data recorded by the dSPACE interface. Its block diagram is shown in Fig. 5. It consists mainly of evaluating and plotting the FRF for each run, recording N selected satisfactory FRFs, and evaluating, plotting and recording the average FRF. In this work, $N = 20$ selected FRFs were used to evaluate the average FRF. A FRF estimator equal to the cross-spectrum, between input (chirp voltage) and output (velocity), divided by the autospectrum of the input was considered. The input and output spectra were obtained using the fast fourier transform algorithm of MATLAB.

3. RESULTS AND DISCUSSION

This section presents some damping performance analyses based on the FRFs obtained for each configuration design and for four selected control gains. In particular, Figs. 6, 7, 8 and 9 show the FRF for the four active-passive damped cantilever beams: EA, APCL, AC/PCL and SAP, respectively. For reference, the first five bending eigenfrequencies for each configuration were evaluated from the FRFs and are shown in Tab. 1. One can notice that the four configurations have similar modal properties, except for the SAP beam, which is stiffer than the other three.

Fig. 6 shows that the velocity feedback control law may yield a significant decrease in the response amplitude at the first and second eigenfrequencies. However, the same performance is not observed at the other eigenfrequencies. In fact, the amplitude at the fifth eigenfrequency increases with the control gain magnitude. This was expected and it is a known

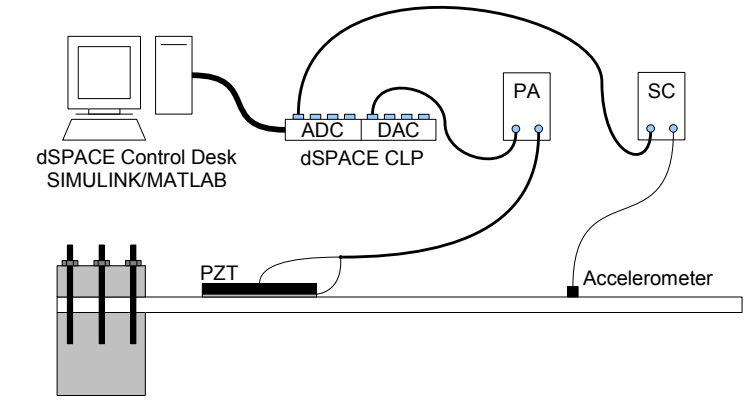

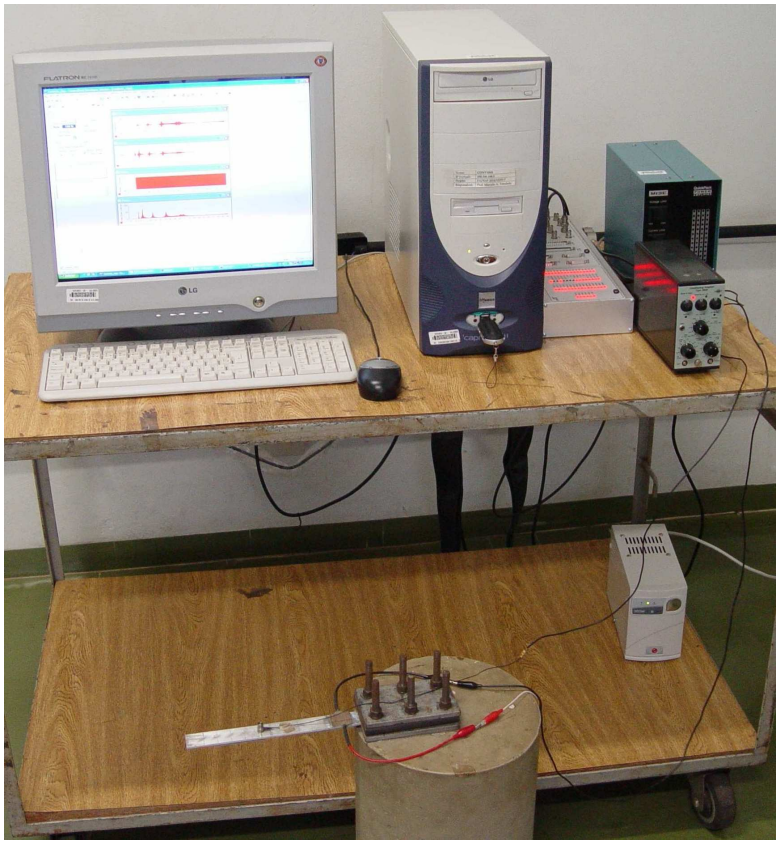

Figure 3. Schematic representation and picture of the experimental setup.

Table 1. First five bending eigenfrequencies (Hz) of the four beam configurations.

	Mode 1	Mode 2	Mode 3	Mode 4	Mode 5
EA	51.9	323	857	1677	2777
APCL	52.0	299	968	1897	2824
AC/PCL	55.0	313	989	1905	2829
SAP	83.1	431	1085	1979	3076

downside of such a simple control law. It may be easier however to analyze the damping performance of this active damping treatment through the modal damping factors for each control gain. They are shown in Tab. 2 for the first five bending modes of the EA damped cantilever beam. Notice that the beam without active damping is represented by $k_0 = 0$, that is with zero control voltage. In this case, the piezoceramic patch acts only as additional mass and stiffness to the beam and, thus, should not improve modal damping. Hence, as expected, very low damping factors (less than 0.4%) were measured for the zero control gain and are attributed mainly to the material damping of the aluminum beam. This case may therefore be used as a reference for the non-treated cantilever beam. As observed in Fig. 6, the first and second modes

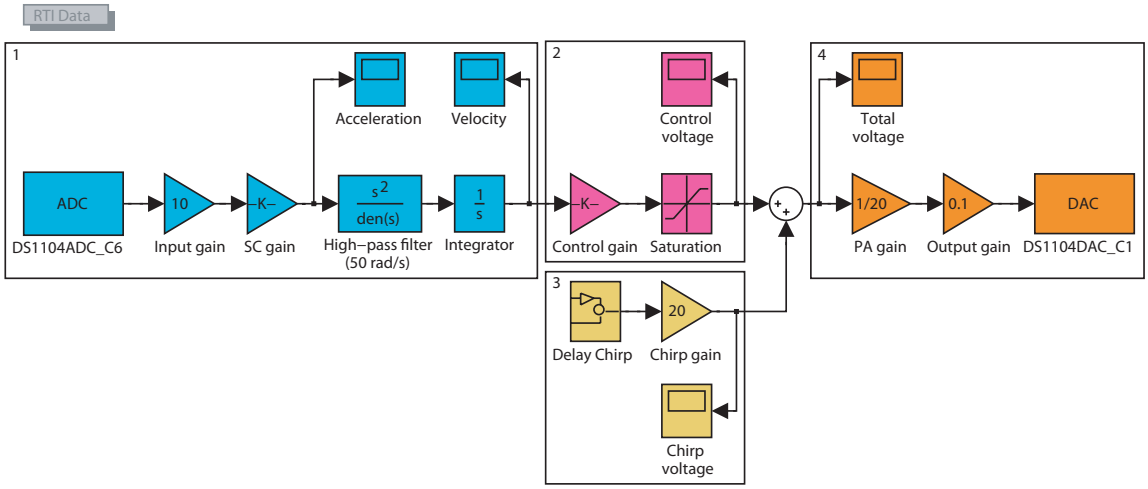

Figure 4. Simulink model used for signal processing and feedback control voltage evaluation.

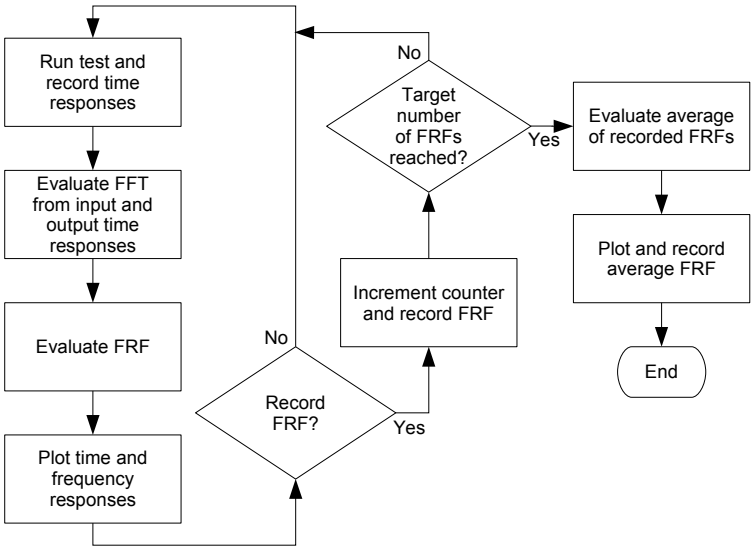

Figure 5. Block diagram of MATLAB program for frequency response function evaluation.

damping factors are significantly increased by the feedback controller, while the fifth mode damping factor has a small overall decrease for the larger control gain. Notice that, as it is well-known for direct velocity feedback controllers, this damping performance is valid only for this selected position of the accelerometer, at 160 mm from the clamp, for which the controller clearly prioritizes the first vibration mode.

The FRF of the APCL damped cantilever beam is shown in Fig. 7. One may notice that, in comparison to the previous case, the relative decrease in the response amplitude with respect to the passive (zero control gain) treatment, when the control gain is increased, is smaller. Some decrease in the response amplitude can be observed though at the first and second resonances. When analyzing the modal damping factor, shown in Tab. 2, this fact can be confirmed. It can also be noticed from Tab. 2 that the APCL treatment has nearly no effect on the third vibration mode and leads to a decrease in the damping factors of the fourth and fifth modes. Again, this is mainly due to the choice of accelerometer position (at 78 mm from the clamp) and different damping factors are obtained for other positions. It is worthwhile noticing however that the passive damping performance of the APCL treatment, that is for $k_0 = 0$, is quite good. This helps leading to a good active-passive damping performance even for the fourth mode, which is excited by the controller but remains reasonably well damped, with 1% damping factor, for the higher control gain.

The next active-passive damping treatment analyzed is the AC/PCL, which has a construction very similar to the APCL one. Fig. 8 shows the FRF for the AC/PCL damped cantilever beam where it can be noticed that the response of the AC/PCL beam is also very similar to the APCL one. It is possible however to observe that the AC/PCL design leads to larger decreases in the response amplitude at resonance, in particular at the second eigenfrequency. This can be confirmed by analysis of the damping factor in Tab. 2. Comparison of APCL and AC/PCL designs damping factors show that, except

for the fifth vibration mode, both configurations yield similar passive damping performances but AC/PCL leads to better active-passive performance. These results confirm that the loss of active transmissibility can be more important than the increase in viscoelastic shearing for APCL treatments. On the other hand, since the piezoceramic patch also acts as a constraining layer stiffener, passive damping performance may be higher for the APCL treatment, compared to AC/PCL one, as observed for the third, fourth and fifth modes in Tab. 2 ($k_0 = 0$).

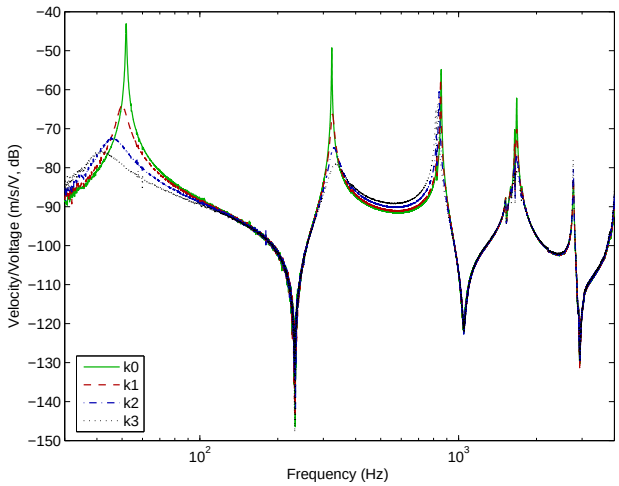

Figure 6. FRF for the EA damped cantilever beam with accelerometer at 160 mm from clamped end for various control gains: $k_0 = 0$, $k_1 = -2$ kVs/m, $k_2 = -6$ kVs/m, $k_3 = -10$ kVs/m.

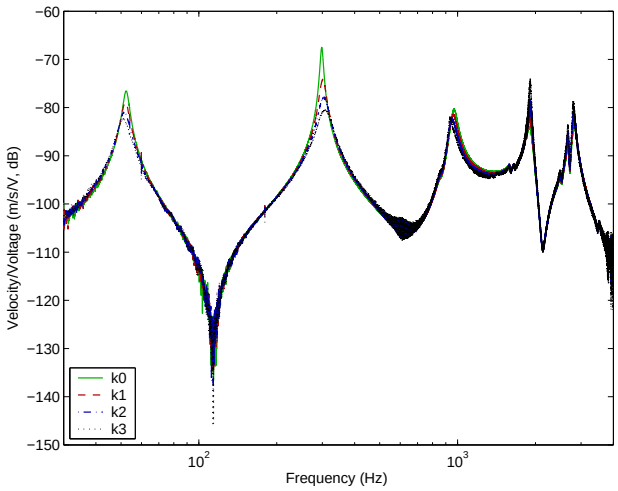

Figure 7. FRF for the APCL damped beam with accelerometer at 78 mm from clamped end for various control gains: $k_0 = 0$, $k_1 = 6$ kVs/m, $k_2 = 12$ kVs/m, $k_3 = 18$ kVs/m.

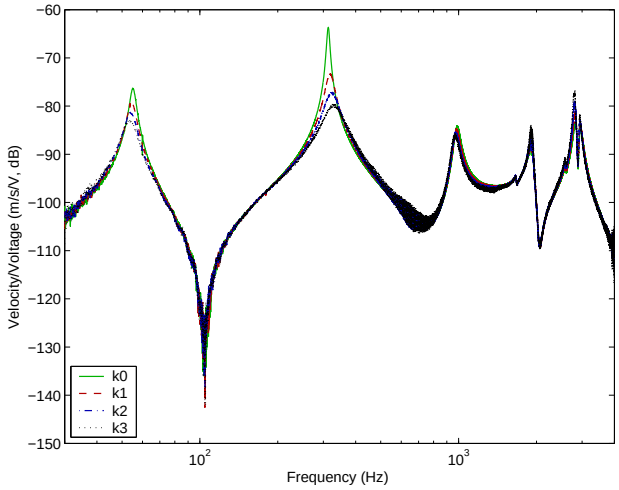

Figure 8. FRF for the AC/PCL damped beam with accelerometer at 78 mm from clamped end for various control gains: $k_0 = 0$, $k_1 = -7$ kVs/m, $k_2 = -13$ kVs/m, $k_3 = -19$ kVs/m.

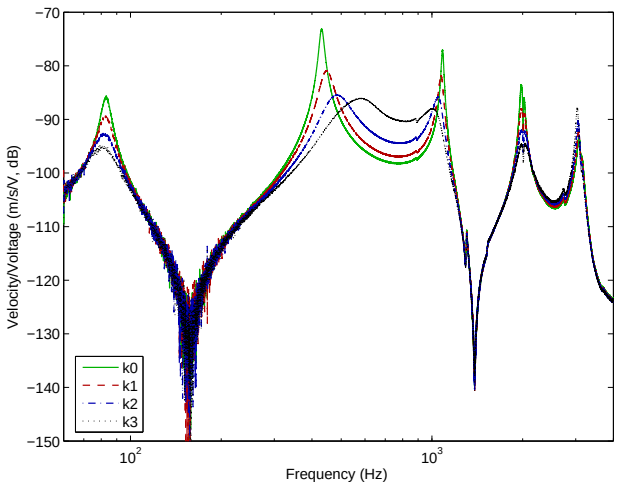

Figure 9. FRF for the SAP damped sandwich beam with accelerometer at 130 mm from clamped end for various control gains: $k_0 = 0$, $k_1 = -10$ kVs/m, $k_2 = -25$ kVs/m, $k_3 = -40$ kVs/m.

Finally, the sandwich shear active-passive (SAP) damped beam is analyzed. From its FRF, shown in Fig. 9, it is possible to observe that a significantly higher decrease in resonant amplitudes can be obtained with this design. Notice however that care should be taken when comparing this design with the other active-passive ones since, in this case, the base structure is quite different. Still, Fig. 9 shows that a significant decrease in the response amplitude can be obtained at the first four eigenfrequencies. This fact is confirmed by the modal damping factors, presented in Tab. 2, where it can be observed that, although the third and fourth modes are less damped passively, large damping factors can be obtained by increasing the control gain. It is also noticeable that the SAP treatment does not affect much the fifth vibration mode.

Besides the active-passive damping performance, it is also worthwhile analyzing the control voltage required to induce such a performance. In order to allow comparison of the four design configurations tested, the following procedure was considered. First, the peak voltages sent to the piezoelectric patch by the velocity feedback controller at the five resonances were observed. Then, the mean control voltage peak was divided by the chirp excitation voltage amplitude. This index

Table 2. Damping factors (%) for the first five bending modes of EA, APCL, AC/PCL and SAP damped beams with various control gains.

	Control gain (kVs/m)	Mode 1	Mode 2	Mode 3	Mode 4	Mode 5
EA	$k_0 = 0$	0.39	0.17	0.16	0.25	0.25
	$k_1 = -2$	4.12	1.29	0.21	0.63	0.32
	$k_2 = -6$	10.9	3.83	0.27	1.20	0.27
	$k_3 = -10$	14.9	6.99	0.33	1.71	0.22
APCL	$k_0 = 0$	2.87	1.29	3.18	3.03	2.23
	$k_1 = 6$	3.87	2.88	3.46	2.11	1.91
	$k_2 = 12$	4.77	4.53	3.59	1.63	1.58
	$k_3 = 18$	5.75	6.08	2.95	0.99	1.32
AC/PCL	$k_0 = 0$	2.82	1.29	2.92	2.86	1.66
	$k_1 = -7$	4.06	4.09	3.14	2.34	1.45
	$k_2 = -13$	5.13	6.52	3.41	2.00	1.23
	$k_3 = -19$	6.76	9.07	3.54	1.64	1.10
SAP	$k_0 = 0$	3.49	1.85	0.90	0.98	1.25
	$k_1 = -10$	5.75	5.22	1.84	1.39	1.18
	$k_2 = -25$	8.17	11.3	4.09	1.90	1.13
	$k_3 = -40$	10.8	18.7	9.91	2.41	1.02

can be interpreted as the mean control effort, normalized by the excitation magnitude, required to yield the corresponding damping performance. This analysis leads to the following indices for the active-passive damping designs: EA - 2.10 V/V, APCL - 2.09 V/V, AC/PCL - 1.80 V/V and SAP - 1.42 V/V. From this result, it seems that a similar control effort is required for EA and APCL treated beams. Thus, the choice between them is more dependent on whether one needs larger damping performance for selected modes (EA), at the expense of other modes damping, or more robust and wide-range, but smaller individual, damping performance (APCL). On the other hand, comparison between APCL and AC/PCL shows that AC/PCL may yield better overall damping performance than APCL with the additional benefit of lower control effort. Finally, for the case studied in this work, the SAP design combines the large damping for selected modes, of EA design, with wide-range and robust damping performance, of APCL and AC/PCL, and, additionally, requires even smaller relative control effort.

4. CONCLUDING REMARKS

This work has presented an experimental analysis of three active-passive damping design configurations applied to a cantilever beam: two design configurations based on the extension mode of piezoelectric actuators combined to viscoelastic constrained layer damping treatments and one design configuration with shear piezoelectric actuators embedded in a sandwich beam with viscoelastic core. For comparison purposes, a purely active design configuration with an extension piezoelectric actuator bonded to an elastic beam was also analyzed. Comparison of the active-passive damping performance yielded by the four design configurations has confirmed that active-passive designs provide more robust, reliable and wider-range damping performance than purely active one. In addition, they may also require smaller control effort.

5. ACKNOWLEDGEMENTS

This research has been financially supported by The State of São Paulo Research Foundation (FAPESP), which is gratefully acknowledged by the authors.

REFERENCES

Azvine, B., Tomlinson, G.R. and Wynne, R., 1995, "Use of active constrained-layer damping for controlling resonant vibration," Smart Materials and Structures, 4(1):1–6.

Badre-Alam, A., Wang, K.W. and Gandhi, F., 1999, "Optimization of enhanced active constrained layer (EACL) treatment on helicopter flexbeams for aeromechanical stability augmentation," Smart Materials and Structures, 8(2):182–196.

Baillargeon, B.P. and Vel, S.S., 2005, "Active vibration suppression of sandwich beams using piezoelectric shear actuators: experiments and numerical simulations," Journal of Intelligent Materials Systems and Structures, 16(6):517–530.

Baz, A. and Ro, J., 1994, "Concept and performance of active constrained layer damping treatments," Sound and Vibration Magazine, pp.18–21.

Baz, A. and Ro, J., 2001, "Vibration control of rotating beams with active constrained layer damping," Smart Materials and Structures, 10(1):112–120.

Chan, K.W. and Liao, W.H., 2006, "Active-passive hybrid piezoelectric actuators for high precision hard disk drive servo systems," in Smart Structures and Materials 2006: Smart Structures and Integrated Systems, Y. Matsuzaki (ed.), Proceedings of SPIE, vol. 6173, no.617303-10.

Chantalakhana, C. and Stanway, R., 2000, "Active constrained layer damping of plate vibrations: A numerical and experimental study of modal controllers," Smart Materials and Structures, 9(6):940–952.

Crassidis, J., Baz, A. and Wereley, N., 2000, "H_∞ control of active constrained layer damping," Journal of Vibration and Control, 6(1):113–136, 2000.

Huang, S.C., Inman, D.J. and Austin, E.M., 1996, "Some design considerations for active and passive constrained layer damping treatments," Smart Materials and Structures, 5(3):301–313.

Kapadia, R.K. and Kawiecki, G., 1997, "Experimental evaluation of segmented active constrained layer damping treatments," Journal of Intelligent Material Systems and Structures, 8(2):103–111.

Lam, M.J., Inman, D.J. and Saunders, W.R., 1998, "Variations of hybrid damping," in Smart Structures and Materials 1998: Passive Damping and Isolation, L.P. Davis (ed.), Vol.3327, pp.32–43, Bellingham (USA), SPIE.

Langote, P.K. and Seshu, P., 2005, "Experimental studies on active vibration control of a beam using hybrid active/passive constrained layer damping treatments," Journal of Vibration and Acoustics, 127:515–518.

Lesieutre, G.A. and Lee, U., 1996, "A finite element for beams having segmented active constrained layers with frequency-dependent viscoelastics," Smart Materials and Structures, 5(5):615–627.

Liao, W.H. and Wang, K.W., 1996, "A new active constrained layer configuration with enhanced boundary actions," Smart Materials and Structures, 5(5):638–648.

Park, C.H. and Baz, A., 2001, "Comparison between finite element formulations of active constrained layer damping using classical and layer-wise laminate theory," Finite Elements in Analysis and Design, 37(1):35–56.

Ray, M.C., Oh, J., and Baz, A., 2001, "Active constrained layer damping of thin cylindrical shells," Journal of Sound and Vibration, 240(5):921–935.

Rongong, J.A., Wright, J.R., Wynne, R.J., and Tomlinson, G.R., 1997, "Modelling of a hybrid constrained layer/piezoceramic approach to active damping," Journal of Vibration and Acoustics, 119(1):120–130.

Trindade, M.A., 2007, "Multiobjective optimization of active-passive damping treatments using genetic algorithms," in Proceedings of the XII International Symposium on Dynamic Problems of Mechanics (DINAME 2007), P.S.Varoto and M.A.Trindade (eds), ABCM, Ilhabela, in CD-ROM.

Trindade, M.A. and Benjeddou, A., 2002, "Hybrid active-passive damping treatments using viscoelastic and piezoelectric materials: review and assessment," Journal of Vibration and Control, 8(6):699–746.

Trindade, M.A., Benjeddou, A. and Ohayon, R., 2001, "Piezoelectric active vibration control of sandwich damped beams," Journal of Sound and Vibration, 246(4):653–677.

Varadan, V.V., Lim, Y.-H., and Varadan, V.K., 1996, "Closed loop finite-element modeling of active/passive damping in structural vibration control," Smart Materials and Structures, 5(5):685–694.

Vasques, C.M.A. and Dias Rodrigues, J., 2007, "Active vibration control of a smart beam through piezoelectric actuation and laser vibrometer sensing: simulation, design and experimental implementation," Smart Materials and Structures, 16:305–316.

Wang, G., Veeramani, S. and Wereley, N.M., 2000, "Analysis of sandwich plates with isotropic face plates and a viscoelastic core," Journal of Vibration and Acoustics, 122:305–312.

Yellin, J.M. and Shen, I.Y., 1996, "Self-sensing active constrained layer damping treatment for a Euler-Bernoulli beam," Smart Materials and Structures, 5(5):628–637.

RESPONSIBILITY NOTICE

The authors are the only responsible for the printed material included in this paper.